DOI: 10.1478/AAPP.103S1A2

AAPP | Atti della Accademia Peloritana dei Pericolanti
Classe di Scienze Fisiche, Matematiche e Naturali
ISSN 1825-1242

Vol. 103, No. S1, A2 (2025)

LIMITATIONS TO CARBON NEUTRALITY OF BIOMASS FUELS

GILBERT AHAMER *

ABSTRACT. For biomass fuels, carbon neutrality has long been assumed, and therefore biomass fuels of various origin play an important role in climate protection strategies. However, a closer look to the involved pools and fluxes of carbon (C) may show a more differentiated picture. For this target, the "Combined Energy and Biosphere Model" CEBM, with 2433 grid elements across the continents, was developed to analyse the net effect of worldwide and extensive usage of biomass as a fuel, replacing fossil fuels. Results suggest that over decades, the C pools of litter and especially soil organic carbon (SOC, i.e., humus layer) decompose considerably as a result of the interrupted natural carbon cycle, when extracting huge amounts of biomass from the natural cycle.

1. Introduction

The causes of climate change have been quantitatively evaluated throughout the previous few decades (Intergovernmental Panel on Climate Change (IPCC) 2021), and the results have been translated into overarching guidelines for international efforts to combat global warming. At the national, supranational, and international levels, several energy systems and fuel groups were favoured while others were not (the most notable recent example being the "European Green Deal"[1]). Given the approximately tenfold larger energy-related GHG (greenhouse gas) emissions from energy as compared to deforestation, energy-related CO_2 emissions constitute the core of all solutions, while deforestation-related emissions played an essential but modest part (T. Abbasi and S. A. Abbasi 2010). While solar energy, including photovoltaics and solar thermal energy, and wind energy typically take the lead in energy strategies, biomass energy sources have historically played a significant role, even if only as "transitory fuel" (Schlamadinger *et al.* 1995; Kraxner, Nilsson, and Obersteiner 2003; Demirbas 2004; Azar *et al.* 2006; Rittmann 2008; Sahin 2011; Muench and Guenther 2013). If only the production of biomass fuels adhered to sustainability recommendations on a number of levels, including how practices and technologies during the growth, harvesting, and conversion phases resulted in additional emissions and adhered to environmental protection standards in general. In that context, biomass energy was commonly regarded as "carbon neutral" from a theoretical standpoint because the resulting

[1] https://ec.europa.eu/info/strategy/priorities-2019-2024/european-green-deal_en

net zero balance of carbon flows was taken to be an accurate representation of reality: precisely the amount of carbon released during growth was taken up by these plants from the atmosphere (Schlamadinger *et al.* 1995; Kraxner, Nilsson, and Obersteiner 2003; Demirbas 2004; Azar *et al.* 2006; Rittmann 2008; T. Abbasi and S. A. Abbasi 2010; Sahin 2011; Muench and Guenther 2013). According to this perspective, emissions produced during the growth, harvest, and conversion of raw biomass into easily burning fuels were the sole factors affecting the carbon neutrality of biomass, and they were therefore considered "secondary effects". In that case, a focused investigation was conducted to confirm the biomass fuels' carbon neutrality hypothesis, that is, to calculate their net impact on the amount of CO_2 in the atmosphere globally, as well as to assess their potential globally. The current text provides more in-depth fundamentals on the model used because a recent article (Ahamer 2022) attracted a lot of interest (Green and Reyes 2023; Kukharets *et al.* 2023; Nastasi *et al.* 2023; Podolets *et al.* 2023; Tran, Juno, and Arunachalam 2023; Tregub 2023; Gürdil, Demirel, and Cevher 2024; Le *et al.* 2024; Sahni, Verma, and Kumar 2024).

2. Materials and Methods

2.1. The quantitative tool: Combined Energy and Biosphere Model (CEBM). The author developed the "Combined Energy and Biosphere Model" (CEBM) as a global carbon cycle model, building upon the previous model OBM (Osnabrück Biosphere Model). The OBM was initially created by Prof. Gerd Esser in Osnabrück and Giessen, Germany (Esser 1984, 1987, 1988). It was further improved at IIASA Laxenburg, Austria, and eventually transformed into the HRBM by G. Esser. The CEBM increased the program size of the previous model OBM by two-fold (Ahamer 1993, pp. 238–259) and incorporates a tool for energy scenarios (Ahamer 1993, Figure 9 therein). The CEBM's biospheric program component enables the calculation of the complete global carbon cycle, encompassing the atmosphere, ocean, standing biomass, litter (fallen leaves and twigs), and soil organic carbon (SOC), across 2433 grid elements worldwide. The primary carbon (C) transfers (facilitating exchange between these carbon reservoirs) consist of yearly plant growth and plant decomposition (influenced by local temperature and precipitation levels) (Ahamer 2019, p. 305). The C fluxes provide a condition of equilibrium that remains constant, which is a common characteristic of all biological systems (Claret, Sonnerup, and Quay 2021). The carbon cycle's global stability is dictated by the magnitudes of the many fluxes that exist, as demonstrated by CEBM model runs. High susceptibility to external disturbances arises when these disturbances constitute a significant proportion of the flows under consideration (Körner 2006; Nickerson and Risk 2009; Wang, Law, and Pak 2010; Wieder, Boehnert, and Bonan 2014; Chen, Lewis, and Xiang 2015; Claret, Sonnerup, and Quay 2021). When the global yearly fossil carbon emissions were entered into the model, it accurately predicted the atmospheric CO_2 concentration as measured in experiments (control runs) (Ahamer 1993, pp. 262–265), acting as an important initial test for its trustworthiness. Subsequently, the model allocated a specific proportion of each grid cell's surface area for the generation of biomass fuels, which could be utilized as a substitute for fossil fuels while maintaining an equivalent energy content for both fuel types. The CEBM accurately models the steady-state equilibria of the global carbon cycle, as shown in Figure 1, and as described in more detail in Annex A. This is done through detailed maps and time series analysis, as

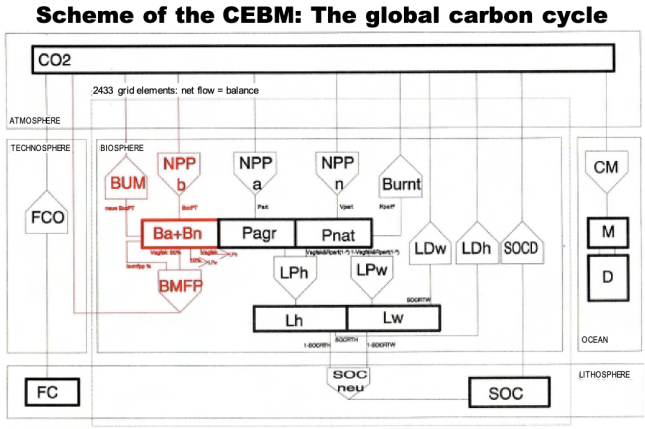

FIGURE 1. The configuration of the worldwide carbon reservoirs (rectangles) and fluxes (arrows) in the CEBM (Ahamer 1993, 2019), calculated on 2433 grid elements. Key: The red program module provides a description of the growth (NPPb) and production (BMFP) of biomass fuels. BUM refers to the biomass that remains on previously used areas and is later employed for the growth of biomass fuels. This biomass may or may not be burned as fuel. Additional sections include: NPP = net primary productivity (in agricultural and natural regions), Burnt = deforestation, L = litter (composed of leaves and twigs), LP = litter production (including herbaceous and woody materials), LD = litter depletion. SOC refers to soil organic carbon, which encompasses both its production (neu) and depletion (D). M & D refer to the mixed and deep layers of the global ocean, while CM represents the net intake of substances by the ocean. FC refers to fossil carbon, while FCO stands for fossil combustion. For a comprehensive list of variables, please refer to Table 3 in the Annex. Reference: Ahamer, 2022.

described in Ahamer (1993, pp. 53–64 and pp. 291-309). As a result, the CEBM effectively models the net impact of increased biomass combustion on biomass fuel usage. This dynamic perspective does not consider a static calculation that only considers two identical global carbon flows: "CO_2 emitted by biomass fuel combustion" and "CO_2 absorbed (or sequestered) by biomass fuel growth". Simply adding up these two carbon flows would result in a net zero, which supports the concept of biomass fuels being theoretically carbon neutral.

2.2. The sensitivities vary greatly: yearly CO_2 emissions, deforestation, and the impact of fertilizers. The preceding article (Ahamer 2022) provides many measurements preceding the primary study inquiry into the "carbon neutrality of biomass fuels." In order to evaluate the sensitivity of various assumptions on the resulting atmospheric CO_2 concentration, several runs of the CEBM model were conducted. These runs assessed the impact of three commonly suggested hypotheses: (1) CO_2 fertilization, (2) deforestation, and (3) fossil CO_2 emissions. The model determined the effect of each of these factors on the projected

atmospheric CO_2 concentration for the year 2100, with the measures ranked in decreasing order of effectiveness.

3. Results

CEBM model runs are conducted using alternative scenario assumptions, employing a "what-if" logic to enable comparisons across scenarios and draw conclusions.

3.1. Scenarios on the amount of biomass fuel production areas. Different sets of biomass (BM) energy scenarios were analysed, with different assumptions on the total area allocated for BM energy production. This led to over 70 test runs of the CEBM. One underlying fact is that humanity undeniably needs naturally occurring areas and specifically agriculturally utilised areas, which together account for 100% in the pre-biomass energy era. However, in the current era of converting biomass into energy, the growth of biomass can only occur by reducing either natural or agricultural areas. Evidently, these alternatives will promptly generate social problems, particularly due to the fact that biomass energy lacks significant energy density.

TABLE 1. The five biomass production types in the CEBM. The abbreviation combines the former area (natural or agricultural: 1st letter) and the form of growth (2nd letter).

Abbreviation	Biomass Production Type
ap	Energy plantations on former agricultural areas
as	Energy utilization of agricultural biomass (e.g. straw burning)
av	Energy plantations on formerly natural areas
nv	Energy use of natural biomass growing on natural areas (age 5 years)
nvn	Energy use of natural biomass growing on natural areas (forestry)

There are two primary categories of biomass production scenarios:

(1) Each year, 0.1% of the area of each grid cell, whether it is natural or agricultural, is allocated for biomass energy production. As a result, after a century, 10% of the initial area will be used for BM fuel production, while still leaving enough space for the original purposes of natural or agricultural vegetation.
(2) Annually, 1% of the area of each grid cell, whether it is natural or agricultural, is allocated for the production of biomass energy. As a result, after one hundred years, the entire initial area will be dedicated to biomass fuel production, leaving no space for the original purposes of the previous natural or agricultural vegetation. It is evident at present that the detrimental impacts on the entire globe in this set of possibilities are excessively powerful to be considered "sustainable" any longer. However, these scenarios are all hypothetical and hence harmless thought experiments conducted to evaluate the global impacts of biomass energy when pushed to its theoretical maximum.

The fundamental message from the four scenario types can apply to both major categories of biomass production scenarios.

(1) The impact on the global atmospheric CO_2 concentration is negligible, hence this "soft" scenario mode provides insufficient assistance in addressing the primary research subject of combating global warming.
(2) Although significant efforts have been made to reduce the greenhouse effect, it is clear that the negative impacts on the entire world are too severe to be considered "sustainable" in any sense. These detrimental impacts encompass significant harm to established land-use change patterns, complete destruction of either agricultural or natural vegetation cover for the sake of energy production, and disruption of ecological and economic processes at all levels. In such situations, the Earth would experience a complete disruption of its natural material cycles, resulting in a significant alteration of planetary biology and further harm to the climate, which was originally intended to be preserved. Hence, the above four modelling scenarios teach: either the mitigating effect of biomass energy on the global greenhouse effect is so small, or if the mitigating effect is large enough, the limits of sustainability are not kept.

3.1.1. *Results from the simulations on the expansion of biomass energy.* The aforementioned scenarios have a collateral impact on five methods of biomass growth, as shown in Table 1. This impact results in the global potential for biomass fuels, which refers to the biosphere's ability to create biomass that can be burned Ahamer (2019, pp. 61–64). The CEBM assumes that only the annually growing biomass is used for combustion, not the standing biomass or phytomass. This is done to incorporate sustainability in a broad sense. The arrow denoting biomass fuel production (BMFP), depicts a flow that intentionally diverts a significant portion of the naturally occurring net primary productivity (NPP), which refers to the annual development of plants.

3.1.2. *Concisely summarizing the impact of biomass strategies on the carbon cycle at a worldwide scale resulting from the Combined Energy and Biosphere Model (CEBM).*. According to the calculations provided, the primary impacts of using biomass for energy on the global carbon cycle are as follows:

(1) There is a reduction in emissions of CO_2 from fossil fuels, although to a lesser extent compared to the emissions produced by biomass fuels. This is because wood, which is a common biomass fuel, has a lower energy value compared to the current mix of coal, oil, and gas.
(2) In certain types of scenarios, the overall amount of plant biomass globally decreases significantly. This is because natural forests naturally store more carbon per unit area compared to dedicated biomass fuel plantations, regardless of the specific strategies employed.
(3) In all types of scenarios, the carbon flow through the litter compartment (as shown in Figure 1) decreases due to the removal of "BM fuels" (flux BMFP in Figure 1) from the area. As a result, the inflow into the soil carbon compartment (SOC in Figure 1) also decreases. The depletion of carbon in this SOC pool is a result of using biomass fuel. In certain instances, the loss is significant. This depletion disrupts the natural global carbon cycle, which has achieved a stable equilibrium over thousands of years. The attainment of this equilibrium can be observed computationally, as demonstrated in Ahamer (1993, pp. 262–263). Over the course

of many years, this phenomenon leads to a significant reduction in the overall amount of organic carbon in the soil (known as humus) on a worldwide scale.

(4) The carbon emissions resulting from the potential conversion of naturally grown areas into ones with decreased forest density must be considered explicitly. These emissions are undesired and quite significant in quantity. Therefore, the main impact of biomass strategies is likely to be the emissions resulting from the reallocation of areas from other dedications to biomass production areas, which can be considered equivalent to deforestation emissions. This finding was unexpected to the author prior to conducting the present study. By 2024, readers are familiar with impactful photographs depicting palm oil plantations in the global South. These plantations have replaced very diverse and densely wooded landscapes that have existed since ancient times (Fitzherbert *et al.* 2008; Danielsen *et al.* 2009; Koh *et al.* 2011; Carlson *et al.* 2013).

(5) The model findings show a clear reduction in the atmospheric CO_2 content, but this reduction is only significant if we fully utilize the theoretical potential for using biomass as an energy source.

(6) The impacts on the global ecology will often be highly significant.

(7) Nevertheless, according to the model output of the CEBM, the utilization of biomass for energy purposes plays a role in decelerating the rise in atmospheric CO_2 levels.

(8) The CEBM is limited to assessing carbon fluxes and cannot evaluate other chemical substances like oxygen, nitrogen, minerals, nutrients, soil quality, biodiversity, or economic parameters. Hence, it is imperative that other considerations be taken into account to supplement the findings of the CEBM. The evaluation of the value of BM methods is likely to be viewed in an even more critical manner.

(9) Interdisciplinary aspects must be considered when assigning additional weight to all relevant consequences.

TABLE 2. Comparison of the CO_2 reduction by 2100 that can be attained through various approaches, as determined quantitatively by CEBM scenarios.

Mitigation Measure (CEBM Scenario)	**Atmospheric CO_2 Content in 2100 (ppm)**	**CO_2 Reduction Compared to Trend Case for 2100**
Trend = The emissions are increasing at a rate of 3% each year due to the rising energy consumption, while everything else remains unchanged.	1200	0
Maximum global biomass utilization (assuming a trend scenario of +3% per year)	1000	150
The mitigation of the rise in emissions or energy consumption from +3% to +1% (baseline scenario)	650	550

Integration of two methodologies (biomass scenario)	550	650
Annual reduction objective of 1%.	450	750

4. Discussion

4.1. On the concept of achieving complete carbon neutrality through the use of biomass energy. The aforementioned outcome can be elucidated in the subsequent manner: As previously stated, the extraction of plant material from an ecosystem over a period of ten years results in a reduction in the amount of carbon stored in the soil, as indicated by the findings of the CEBM. This is illustrated in Figure 1 and Figure 7. Ultimately, these emissions, including deforestation emissions and fossil CO_2 emissions, are primarily dispersed across the atmosphere and the ocean, similar to other human-caused emissions. When examining the quantity of "net CO_2 emissions from global soils," it is shown that this effect, depending on the model employed, accounts for around half of the energy sources conserved. However, the particular type of biomass growth strategy (referred to as nvn) has a significant role in determining this outcome. The "net emissions from the soil" occur because the flow from the soil organic carbon decomposition (SOCD) pool remains constant due to the consistent activity of microorganisms, but the input into the soil carbon reservoir (SOCneu) decreases by an amount equal to the removal of biomass fuels. The latter is no longer able to follow its "natural" path of "existing litter => soil organic carbon". In general, the intensive production of biomass using high levels of energy constitutes a significant redirection of carbon fluxes on a worldwide scale. This has an impact on the stable balance of carbon movement across carbon reservoirs that have not been extensively affected before. Humans utilise these carbon streams to produce energy, which consequently renders them unavailable to nature for the adequate synthesis of humus (SOC), as indicated by the model findings. It is important to emphasise that the specific magnitude of the soil carbon depletion effect in this situation is determined by the mathematical formula used to measure its degradation. The formula described in (Ahamer, 1993) is considered empirical or heuristic and may not be universally applicable. Generally, it is possible that the numerical applicability of the modelling results from the CEBM may not be perfect. However, based on the existing understanding, it is a reality that a carbon depletion impact does occur, and it is highly likely that its significance in the long run is not insignificant. The conclusion obtained here exhibits a greater level of certainty in terms of its actual existence, but a lesser level of certainty in terms of its quantitative magnitude. It is important to reiterate that in the given scenarios, the assumption was made that natural woody plant growth will be used for burning on a global scale. To mitigate the impact of the biosphere's net CO_2 emission, a possible solution would be to reduce the reliance on biomass for energy. These possibilities have a little impact on the earth's environment, but they only provide a small contribution to reducing the growth in atmospheric CO_2 concentration. It is indeed feasible to utilize cultivation kinds other than "forestry" from the five options indicated in Table 1. Nevertheless, there are two factors that must be taken into account: One method, known as the "nvn" (forestry) method, allows for the preservation of existing biomass during fuel production, thereby avoiding land conversion emissions. However, other scenario types

have a much lower potential for generating fuel. This indicates that the possibility for reducing global greenhouse gas emissions through other types of agriculture (such as av, as, nv, ap) is significantly lower.

4.2. How to accurately delineate system boundaries while identifying steady state equilibria. If one attempts to provide an outcome elevated to a more abstract level, one could make the following argument: Biomass is considered a carbon-neutral fuel because the amount of carbon released during combustion is equal to the amount of carbon absorbed during growth. This balance results in zero net emissions. From this viewpoint, a self-contained system of materials is observed. The act of conceptualizing involved establishing a system boundary that encompassed solely these two fluxes, perceiving this subset of the whole carbon cycle as an independent and self-contained entity. However, upon closer analysis of the biospheric processes, it becomes evident that when global biomass is extensively used for energy, it not only activates a single closed carbon cycle, but also disrupts other pre-existing carbon cycles. These currently disrupted or diminished cycles result in a change in the relatively steady flow balance that has been established over extensive durations. To put it simply, when we expand the scope of observation, we observe shifts in the overall distribution of matter, which are directly linked to significant human impacts on the environment. The initial method of observing the modified steady state equilibria did not allow for the recognition of those. This example highlights the significance of accurately defining the boundaries of a system and being cognizant of the constraints that such a choice imposes on the ultimate outcome of that deliberation. The level of certainty of the model outputs varies depending on the number of considerations taken into account. In this case, it is important to note that the current project's analysis of the potential side effects, effects, and conditions of a worldwide use of biomass for energy is insufficient to fully characterise the wide range of impacts on various aspects of life. Specifically, there is a strong need for economic, social studies, and ecosystem research.

5. Summary

Research findings indicate that extensive utilization of biomass for energy leads to a significant reduction in global carbon stocks, particularly in litter (such as twigs and leaves) and soil organic carbon (specifically, the humus layer). This depletion occurs due to the disruption of the natural carbon cycle. In light of this discovery, the previous theoretical belief in the carbon neutrality of biomass fuels is disproven and may be revised to indicate that they are only half as carbon neutral as previously thought, even in a theoretical context, when compared to the existing fuel mix. It is important to note that secondary emissions, such as those associated with production, transportation, and conversion into biomass fuels, would further undermine the already partial carbon neutrality of biomass. This project also aims to offer decision-making assistance for energy planning. Henceforth, the subsequent lines will employ the modelling outcomes to deduce the appropriate course of action for energy policy makers in a developed nation. Considering the established objectives of (a) meeting energy needs (including reducing demands), (b) ensuring economic efficiency (supply security), and (c) promoting environmental and social compatibility, *e.g.* public acceptance (BMHGI 1984; Spitzer 1990), while also fulfilling its responsibilities in light of the legitimate concern regarding the greenhouse effect. In this setting, the primary focus is

clearly on reducing the energy demand rather than meeting that demand with any type of fuel, including somewhat environmentally friendly biomass fuels. Research has demonstrated that biomass energy carriers have the capacity to reach their theoretical maximum values, namely a gross heat value that is comparable to the current global energy demand, which is surprisingly little. This conclusion necessitates the exploration of other potentials, including energy conservation. Compared to the utilization of C-free (or any) energy sources, the benefit of reducing the energy demand is that it eliminates the need to initiate any form of material flow using the energy being supplied. When selecting energy sources from the "non-carbon" category, it is imperative to exclusively consider environmentally and socially acceptable options. For information on the anticipated and unforeseen releases of different energy technologies, particularly nuclear, refer to the study by Ahamer (2013). Consequently, the current article does not endorse or advocate for nuclear energy. The fight against global warming can only be successful through a combination of diverse energy strategies, as supported by various studies (Akimoto *et al.* 2004; Weiss *et al.* 2007; Ackerman *et al.* 2009; Chester, Horvath, and Madanat 2010; Nordhaus 2011; Pereira Jr. *et al.* 2011; White 2012; Notter, Meyer, and Althaus 2013; Röös *et al.* 2013; Suberu, Bashir, and Mustafa 2013; Gunatilake, Roland-Holst, and Sugiyarto 2014; Moumen *et al.* 2016; Pan *et al.* 2016; Makky *et al.* 2017).. Considering the limits indicated above, which are already based on a global model that only considers the carbon cycle, biomass energy has the potential to play a significant part in a set of measures. However, its impact may be rather small in terms of scale.

The research issue of this article focuses on the comparative significance of biomass energy as a technique for reducing CO_2 emissions. This can be understood in two different contexts:

- Is it advisable to actively encourage the utilization of biomass for sustainable and localized energy production? Affirmative. There is no doubt about the beneficial impact of biomass fuels as a replacement for fossil fuels. The energetic use of biomass has several good side effects, including improving the agricultural revenue structure and reducing foreign dependency. These additional benefits make this method highly desirable. Preventing the depletion of soil humus and promoting sustainable use are crucial.
- Is it possible for the exclusive utilization of biomass fuels to effectively halt the global rise in atmospheric CO_2 levels? Negative. The worldwide capacity for biomass fuels is insufficient for this. Furthermore, research has demonstrated that the utilization of biomass for energy purposes is not completely carbon dioxide-neutral.

Appendix A.

This annex provides more background material describing the sensitivities in the program CEBM, as suggested by reviewers.

A.**1. Temporal and geographical representation of the most important model variables.** In this section, typical results of the "Combined Energy and Biosphere Model" CEBM will be pictured in the subsequent figures while using the example of a standard run that covers the period from 1860 to 2100. These additional scenario runs are based on (i) a scenario

with a low level of deforestation in Ahamer *et al.* (1991)[see Figure 17]; and in Ahamer (2024b)[see Figure 13] and (ii) on a "business-as-usual" (b.-a.-u.) scenario (meaning +3%/a in CO_2 emissions) in the energy industry from the 1980s onwards. On the following pages, the timelines and maps of the most important output variables are given (a selection of them is displayed in Table 3 and Table 4, respectively), which represent the global totals of the most important carbon reservoirs and flows, which are shown in their context in Figure 1.

TABLE 3. List of key variables from the CEBM, showing global totals as timelines:

hline **Variable**	**Unit**	**Designation**
ALZERO	Gt C	Global inventory decline at the beginning of the year
ALNEW	Gt C	Global reservoir of inventory waste at the end of the year
CO_2	ppm vol	CO_2 concentration in the atmosphere
ASFCO	Gt C	Fossil emissions accumulated over the years
ASPHYT	Gt C	Global phytomass
ASNPP	Gt/a C	Global net primary productivity
ASLP	Gt/a C	Global inventory waste production (litter production)
ASLD	Gt/a C	Globally decomposed inventory waste (litter depletion)
ASM	Gt C	Increase in the oceanic mixing layer accumulated over the years since 1860
ASD	Gt C	Accumulated increase in the oceanic depth layer since 1860
ASMD	Gt C	Accumulated increase in the total ocean since 1860
SPVTO	Gt C	Global natural phytomass
SPATO	Gt C	Global agricultural phytomass
SNPV	Gt/a C	Global production of natural phytomass
SNPA	Gt/a C	Global production of agricultural phytomass
SDPHYT	Gt/a C	Globally cleared phytomass
TOTPH	Gt C	Emissions from cleared phytomass accumulated over the years since 1860
ASOC	Gt C	Global reservoir of soil organic carbon at the beginning of the year
ASOCN	Gt C	Global reservoir of soil organic carbon at the end of the year
ASOCD	Gt/a C	Global soil organic carbon depletion
ABURNT	Gt/a C	Global total of cleared biomass
ACSUM	Gt/a C	Global balance of the atmosphere $\rightarrow$ biosphere flow
AFCO	Gt/a C	Annual fossil CO_2 emissions
BSNP_	Gt/a C	Global production of phytomass for energy use
BSPTO	Gt C	Globally existing phytomass for energetic utilization
BACO	Gt/a C	Annual CO_2 emissions from biomass
RASFCO	Gt C	Remaining fossil deposit
CO_2 Gt	Gt C	CO_2 in the atmosphere in Gt

TABLE 4. List of other variables from the CEBM, showing geographic differentiation in maps:

Variable	**Unit**	**Designation**
PVG	g C/m²	Density of natural phytomass
PAG	g C/m²	Agricultural phytomass density
NPV	g C/m².a	Density of productivity for natural phytomass
NPA	g C/m².a	Density of productivity for agricultural phytomass
ACO	Mt C/a	Carbon balance: atmosphere -> biosphere per grid element
DPHYT	Mt C/a	Cleared biomass per grid element

Variable	Unit	Designation
ALH	g C/m²	Density of herbaceous stand waste
ALW	g C/m²	Density of woody stand waste
AP	g C/m²	Density of total phytomass
ANPPPQ	g C/m².a	Density of productivity for the total phytomass
ASOCPQ	g C/m²	Soil organic carbon density
GNP	g C/m².a	Density of productivity for the energetically dedicated phytomass
BPG	g C/m²	Density of energetically dedicated phytomass
PT	% /100	Proportion of agricultural area in the grid element
VPT	% /100	Proportion of natural area in the grid element
RPT	% /100	Proportion of cleared area in the grid element
BAPT	% /100	Share of biomass plantation on former agricultural land
BASPT	% /100	Proportion of agricultural area used for energy (straw)
BAVPT	% /100	Proportion of biomass plantation on former natural area
BNVPT	% /100	Proportion of natural area used for energy (forestry)
BMFP	g C/m².a	Density of the resulting biomass fuel
BUM	g C/m².a	Density of the resulting biomass as a result of conversion into energy areas

In addition to the "+3%/a b.-a.-u. energy scenario", the course of these variables is shown (each as a thinner line) assuming a lower annual global growth rate of fossil CO_2 emissions (namely +1% per year in the low-emissions scenario compared to +3% per year in the trend or "business-as-usual" scenario). This comparison the reader to gain an impression of the magnitudes and sensitivities involved in the global carbon cycle. The main difference between the two curves lies in the different degrees of fertilization effect and the resulting consequences for biospheric variables.

A.**2. The atmospheric CO_2 concentration.** This CEBM variable "CO_2 " for the CO_2 concentration in the earth's atmosphere is provided in parts per million – based on the gas volume (ppm vol, while, in order to convert the atmospheric CO_2 concentration in [ppm] into the carbon content of the atmosphere in [Gt C] for comparison purposes, a multiplication by a factor of 2.11 is necessary). If one continues the modelling exercise the current trend of increasing contemporary annual CO_2 emissions until the year 2100 (with an averaged 3% increase in emissions per year, thus roughly a b.a.u. scenario), this will result in an increase in the atmospheric CO_2 concentration that looks similar to an exponential curve (Figure 2). It reaches even the extremely high value of 1,200 ppm in the year 2100 and hits the not only critical but certainly very dangerous climate reference value of 580 ppm between the years 2040 and 2050. The latter concentration corresponds to twice the so-called pre-industrial concentration (labelled "2 x CO_2 " in Figure 2) and is associated (according to several climate researchers) with an average warming of the Earth's mean temperature of 2 to 4°C, hence should be decisively avoided.

A.**3. Annual fossil CO_2 emissions.** In the trend scenario, the energy industry's fossil CO_2 emissions reach a value of 29 Gt C/a around 2050 and a value of 53 Gt C/a in 2100 (Figure 3, variable AFCO). The effect of the exhaustion of the fossil deposits, which are assumed to be 6,600 Gt C, is already evident (Spitzer 1991; Intergovernmental Panel on Climate Change (IPCC) 2023). For already this reason, in this scenario, towards the end of this 21st century, emissions will only increase more slowly and mathematically correspond to the shape of a Gaussian curve. The emission increase rate of 3% per year that serves for

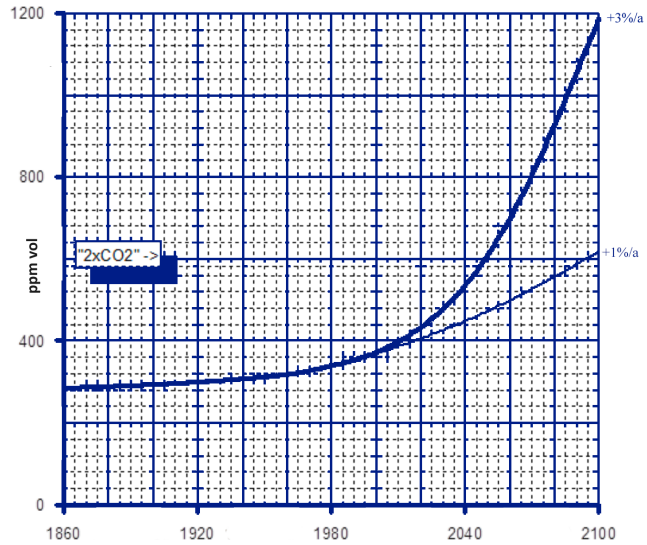

FIGURE 2. The calculated atmospheric CO_2 concentration as a result of the trend (+3%/a) and low emission (+1%/a) scenarios. The undesirable value "2 x CO_2 " is exceeded both times.

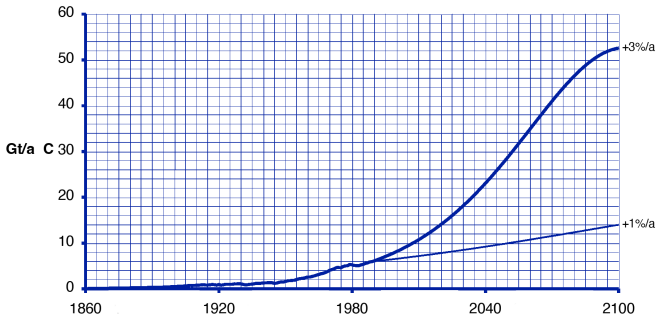

FIGURE 3. The annual energy-related CO_2 emissions for the trend and low-emissions scenarios (+3%/a and +1%/a respectively, taking into account the limited storage facilities, see text).

labelling therefore only applies unchanged at the beginning of the scenarios. Compared to much of the literature (Intergovernmental Panel on Climate Change (IPCC) 1991, 2000), this is a high emissions scenario.

Compare the representation of the variable ASFCO in Figure 4, which indicates the total amount of fossil carbon emitted over the course of history, i.e. represents the time integral

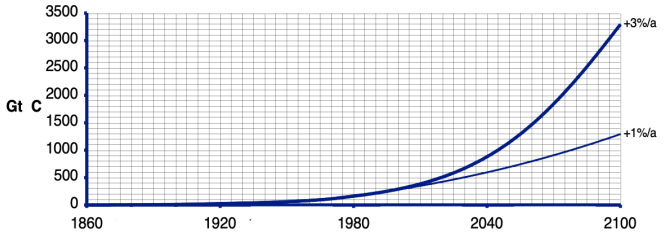

FIGURE 4. The total energy-related amounts of CO_2 emitted from 1860 to the year in question for the trend and low-emission scenarios.

of the previous variable. In the trend scenario, the total amount of fossil fuels emitted from 1860 to 2050 amounts to 1,150 Gt C, and by 2100 this amount will increase to 3,300 Gt C. In contrast, in the low-emissions scenario, emissions rise to only 10 Gt C/a in 2050 or to 14 Gt C/a Gt in 2100, which results in a cumulative value of 1,300 Gt C by the end of the 21st century.

A.**4. Global phytomass (natural and agricultural plant mass).** As can already be seen from the two-colour carbon cycle diagram (Figure 1), the phytomass reservoir (variable ASPHYT) is the result of many inflows and outflows: the quantity of inflowing net primary productivity (NPP) depends on the fertilization effect, and also clearly on the distribution of the area shares between agricultural and natural areas, which can be reallocated through deforestation activities. The latter determines the value of the variable BURNT, which indicates the amount of carbon emitted directly into the atmosphere through slash-and-burn agriculture. The litter production flow also reacts sensitively to deforestation processes because part of the plant mass remains on the ground after the burning process. All of the mentioned carbon flows are of course also influenced by biomass fuel production activities. According to the CEBM model data, the value of phytomass has been falling continuously since 1860 from around 670 Gt C to 635 Gt C (see Figure 5), which can be attributed to historical deforestation processes. Only then this value increases again, which is due to the fact that the ongoing clearing processes taken into account in the model are overcompensated by the more noticeable CO_2 fertilizer effect. The amount of carbon bound in living plant material is currently around 650 to 660 Gt; it is shown in the CEBM as slowly increasing until the year 2050. This increase is due to the fertilizer effect that is effective despite (relatively moderate) clearing activity. From 2050, deforestation will dominate here. In stronger deforestation scenarios, the global phytomass would decrease because the deforestation would no longer be overcompensated by the fertilization effect. It should be noted here that a more severe deforestation scenario would also be plausible (Ahamer 2024b, see Figure 13).

If the total global phytomass is broken down into natural and agricultural phytomass, it is expected that there has been a constant increase in agricultural phytomass (variable SPATO, Figure 6) over the last century from about 0.5 Gt C in 1860 to currently 3.5 Gt C and up to 4-5 Gt C in 2100, depending on the clearing scenario chosen (Ahamer 2024b, see Figure 13). In reality, the extent of agricultural plant mass would of course be very strongly

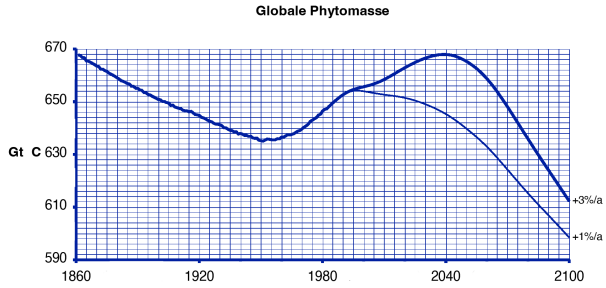

FIGURE 5. The global phytomass (= sum of natural and agricultural plant mass) for the trend and low emission scenarios.

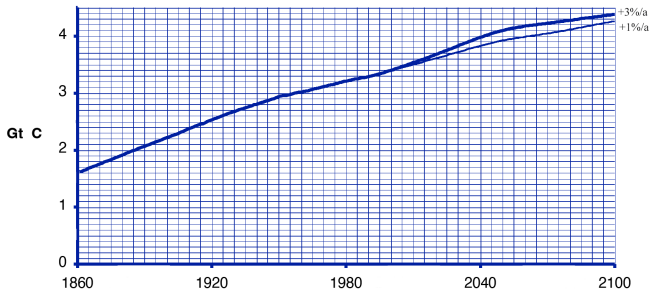

FIGURE 6. The agricultural plant mass for the trend and low emission scenarios

influenced by population development. The curve of the natural plant mass itself (variable SPVTO, not shown) corresponds approximately to the total phytomass.

A.**5. Net primary productivity (NPP).** This mass flow NPP, which describes plant growth, represents the actual carbon pump in the ecosystem. It is controlled by the local temperature and local precipitation as well as by the CO_2 concentration of the atmosphere (Ahamer 2024b, see Figure 4). The allocation of areas to natural or agricultural usage in the relevant grid results into the different algorithms for agricultural and natural net primary productivity and therefore also has a major influence on the final result of the global sum of annual plant growth (variable ASNPP), the timeline in Figure 7. The shape of the curve is similar to that for global phytomass. The annual global flow of carbon is around 40 to 45 Gt C/a. Due to

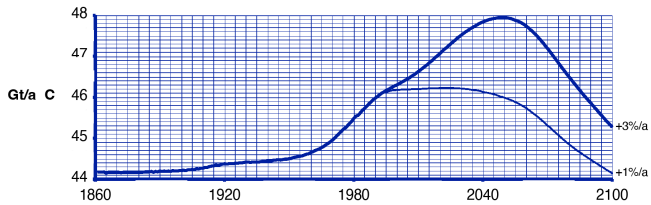

FIGURE 7. The global sum of net primary productivity of natural and agricultural phytomass for the trend and low emission scenarios

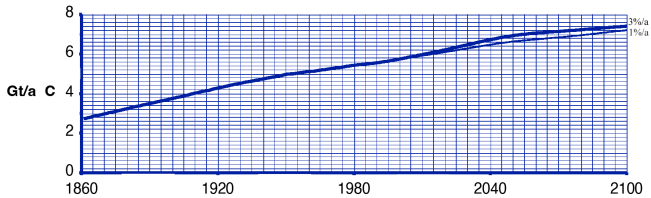

FIGURE 8. The net primary productivity of agricultural phytomass for the trend and low emission scenarios

the CO_2 fertilizer effect, which even outweighs the deforestation activities in this moderate deforestation scenario used, global net primary productivity will even increase until the middle of this century.

If the NPP is separated into agricultural and natural phytomass, it can be seen that the latter reflects the curve of the total phytomass already discussed (variable SNPV, not shown). At the turn of the last century, plant production decreased due to the already existing strong clearing activity, but from around the middle of the current century, while the clearing activity remained approximately the same, the increase in growth due to the fertilizer effect became more prominent, so that the curve turned upwards. The global production of agricultural phytomass (variable SNPA, Figure 8) increases continuously from about 3 to 7 Gt C/a over the entire modelled period. This is understandable because in the CEBM any deforestation activity corresponds to a conversion from natural to agricultural land and consequently the agriculturally used land is constantly increasing over the decades. In addition, the agricultural NPP is also exposed to the CO_2 fertilizer effect, but this only has a very small effect compared to other factors.

A.**6. The reservoir litter including its inflow and outflow.** This reservoir, which is small compared to the streams flowing through it, remains approximately constant over the course of the modelled history, but will increase by around 10 Gt C in the coming century due to the expected deforestation activity (variable ALNEU, Figure 9). This at first glance somewhat surprising increase in all variables associated with the population decline in the next century is the result of the plant masses that were not burned directly, but remained dead on the sites of clearing.

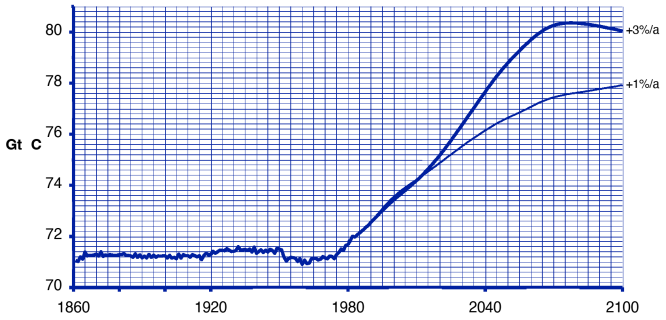

FIGURE 9. The global litter pool (i.e., herbaceous and woody dead plant matter) for the trend and low emission scenarios

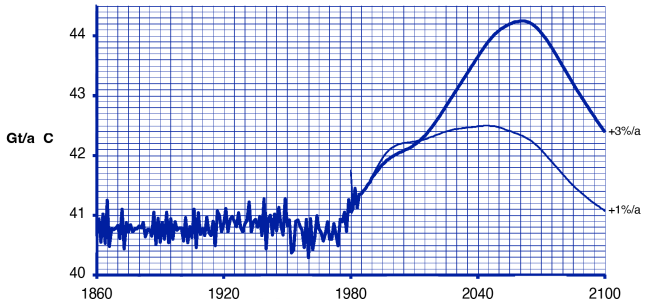

FIGURE 10. The global litter production for the trend and low-emission scenarios.

As Figure 10 shows, the litter production (variable ASLP) amounts to around 40 Gt C/a, with the small spikes in the curve resulting from the discontinuous clearing activities assumed over the last century. Due to the fact that only part of the cleared biomass is burned directly, the other part becomes dead plant mass in the model, i.e. litter, and thus explains the shape of the curve after oscillating deforestation activities.

The global litter depletion flux (i.e., decomposed litter, variable ASLD, see Figure 11), fluctuates around 30 to 35 Gt C/a over the years.

A.**7. Soil organic carbon (SOC).** This reservoir took the longest time to reach the steady state of a stable flow equilibrium during the initial runs describing pre-history (see Ahamer, 2024b: Figure 6). Here the flows are very small compared to the filling level of the reservoir, therefore the picture (in the sense of the dynamic behaviour in a systems-dynamic sense, cf. Boykova, Knyazeva, and Salazkin (2023)) is completely different (namely acting like a buffer, thus showing little flux compared to high filling levels) to that of the previously discussed litter reservoir (namely being very sensitive to flux changes because of the low filling height of the pool). Given these characteristics, one could view the quotient "reservoir size by flux size" as a measure of the dynamic behaviour of the reservoir in

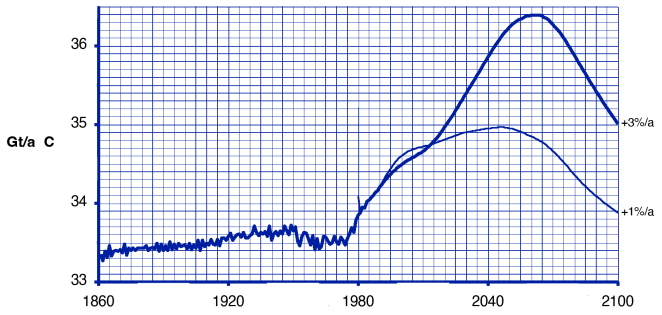

FIGURE 11. The globally depleted litter (litter depletion) for the trend and low-emission scenarios.

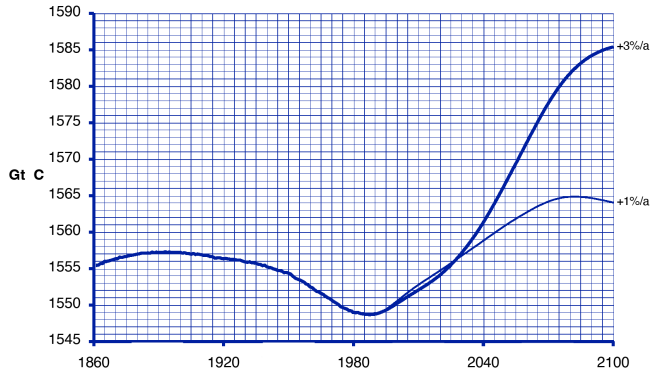

FIGURE 12. The global soil organic carbon (SOC) pool for the trend and low emissions scenarios.

question throughout the carbon cycle. The quantity obtained in this way has the dimension "time" and indicates a kind of reaction time (or relaxation time, to use a term from physics) to sudden changes in flow. Therefore, this quotient could represent a kind of characteristic time constant. The level of the global reservoir of soil organic carbon (variable ASOCN) increased slightly after 1860 due to the onset of deforestation activity, as Figure 12 shows. In contrast to the litter reservoir, the carbon pulse created by clearing activity does not flow through here, but rather stays here for a longer period of time due to the inertia of the reservoir. "Soil carbon" is therefore a metastable, i.e. almost stable, intermediate storage in the system of the global carbon cycle.

In the present calculation model, global soil carbon continuously decreased by a total of almost ten Gt C during the 20^{rh} century. This is due to the reduced inflow into the global humus layer (variable SOCNEU, not shown) and is ultimately a result of the globally lower phytomass due to clearing activities, as can be seen in Figure 5 above. The fact that the decline in global phytomass is subsequently so clearly visible in the soil carbon reservoir,

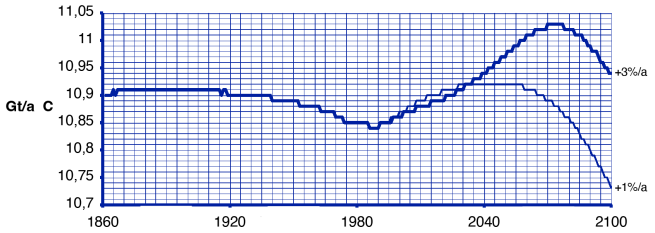

FIGURE 13. The annually globally depleted soil organic carbon for the trend and low-emission scenarios.

while it is much less noticeable in the litter reservoir, can also be viewed as a result of the various "time constants" described above. In other words, it is also due to the large difference in the absolute filling level of the two reservoirs. The flow ASOCD, the global soil carbon depletion, also shows this timeline (Figure 13).

In summary, it should be emphasized again that global soil carbon is a long-term buffer that reacts slowly to changes in the overall system and thus exerts an overall stabilizing effect.

A.**8. The deforested phytomass.** According to the CEBM database, the living plant matter destroyed annually by deforestation (variable SDPHYT, with a negative sign for mathematical reasons) is around the value of around 0.8 Gt C/a, as can be seen from Figure 14. The strong irregularities that are visible are due to annual fluctuations in deforestation activity. In order to assess the effects of deforestation processes in the future, eight scenarios are provided for in the CEBM, which are explained in detail in Ahamer (2024a, see Figure 14). In the present article, the most moderate clearing scenario number 5 is used for all CEBM calculations. Its relationship to other clearing scenarios can be clearly seen in Ahamer (2024b, see Figure 13).(However, only the directly burned plant parts are listed there, which make up around a third of the total cleared plant mass. However, the ratio of the eight curves to one another remains the same for the variable “Globally cleared phytomass”). The undulating timeline over the next century is a result of the combination of the clearing probability on the individual grid elements, which is assumed, among other things, to be proportional to the clearing activity in the neighbouring cells. As can be seen in Ahamer (2019, p. 293), the historical clearing data of the OBM are rather low when compared to the literature. However, from what was said in Ahamer (2019, pp. 50, 295), it is clear that the choice of different clearing scenarios has no significant or even distorting influence on the final result of this overall energy economic analysis, because the theoretical maximum amount of carbon that can be released through deforestation is 660 Gt C (= total plant mass on earth) which is ten times less than the theoretically releasable approx. 6,600 Gt C of the Earth’s fossil reserves.

Also shown graphically in Figure 15 is the flow of direct emissions from plant mass burned to produce CO_2 (variable BURNT), which has the same rhythm of variation. It is anchored in the CEBM that half of the herbaceous plant material and 30% of the woody,

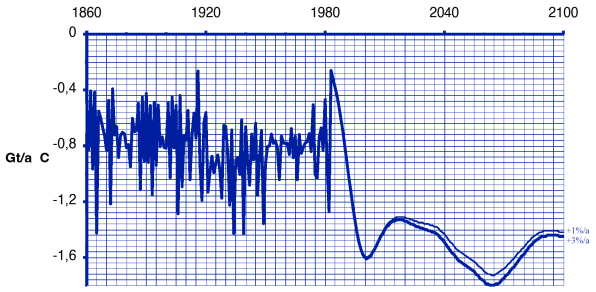

FIGURE 14. The annually deforested phytomass for the trend and low-emission scenarios.

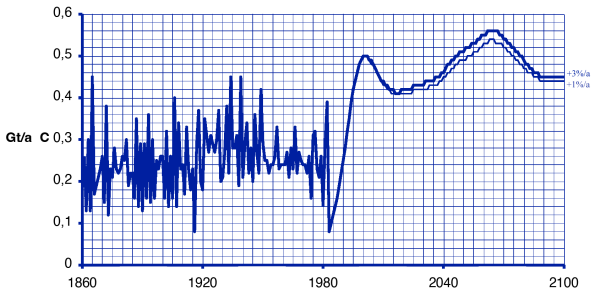

FIGURE 15. The biomass burned annually through deforestation for the trend and low-emission scenarios.

cleared plant material burn directly (Burnt in the carbon cycle diagram in Figure 1), while the rest takes the degradation path via litter.

The global sum of all plant material cleared up to a given year is given by the variable TOTPH, with the year 1860 arbitrarily set as the zero point for the temporal summation

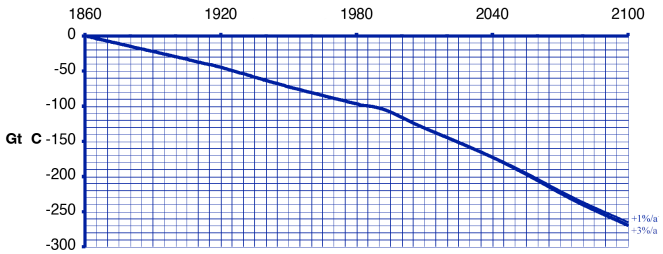

FIGURE 16. The phytomass destroyed globally by deforestation since 1860 for the trend and low ¬emission scenarios.

(arithmetically with a negative sign, see Figure 16). During the 120 years up to present, almost 150 Gt of C plant mass was deforested, if one follows the CEBM database.

A regional differentiation of these historical clearing activities is explained country by country in Ahamer (2019, pp. 48, 293). Interestingly, the picture that emerges is that different areas of the world experience maximum deforestation activity at different times. Regions that have been inhabited for several millennia, such as Europe or China, recorded the maximum of these activities in the last century, during which time they are currently in some cases even switching to reforestation (cf. bright spots in Ahamer (2019, pp. 45–51)). The group of countries known as the “early colonies” of North America and the Soviet Union recorded maximum deforestation around 1900. Finally, the third group of countries, "New Countries", which make up the rest of the world, especially the Third World, shows a sharply increasing trend in deforestation, which is currently reaching its maximum and will possibly continue to increase. It could be that certain historical cycles determine clearing activities. (It remains to be hoped that historical cycles will come into force in a similar way for fossil emissions and that they will decrease again in the future.)

A.**9. Global balance of carbon flows from the atmosphere to the biosphere.** The sum of the flows of "net primary productivity" on natural, agricultural and energy -production areas minus the sum of the flows of inventory waste reduction, soil carbon reduction, slash and burn, BUM (originally existing plant cover resulting from the conversion into energy production areas) is representing a net-balancing variable (see Figure 1 as a flow diagram). In the CEBM, this flow variable is called "Balance" for each grid element and its global sum is output annually as the variable ACSUM. The course of the latter is shown in Figure 17. This quantity can be viewed as net biospheric emission. This parameter includes all deforestation effects as well as effects due to the conversion of natural or agricultural areas into energy production areas. This balance variable, however, does not include fossil emissions or the exchange of CO_2 with the ocean. In the flow diagram of Figure 1, this variable "balance" corresponds to the entirety of all flows that hit the atmosphere, except for the fossil emissions shown on the far left and the uptake by the ocean shown on the far right.

The numerical value for the sum of biospheric emissions was around +0.4 Gt C/a up to 1980, which can be attributed to clearing activities. It may even reach negative values by the end of the next century because the fertilization effect can outweigh the clearing

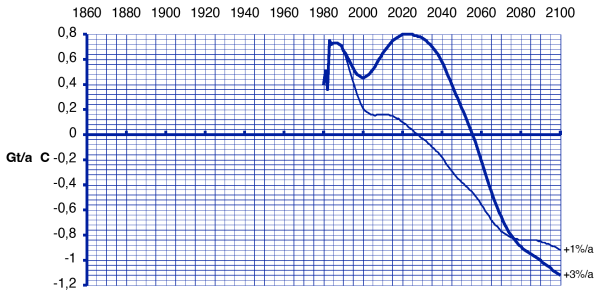

FIGURE 17. The global balance of the flow from the atmosphere to the biosphere for the trend and low-emissions scenarios.

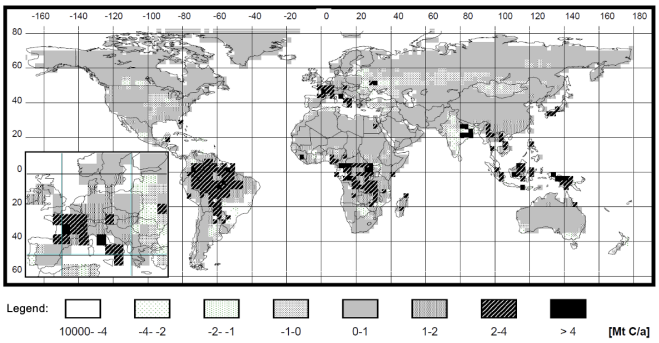

FIGURE 18. The global balance of the flow from the atmosphere to the biosphere at present as a map. Source: CEBM.

processes. A global distribution of biospheric emissions is shown in the map of Figure 18, with areas with strong deforestation activity (shown dark; for example, the tropical rainforest) separated from those with reforestation activity or a strong CO_2 fertilization effect (shown light; for example USA, China) can be distinguished. Neutral areas are shown in grey.

It should be noted that this variable "carbon balance on the grid elements" is the most sensitive of all output variables to biospheric processes and that its numerical value represents a sensitive measuring needle for indicating changes in the biospheric carbon balance.

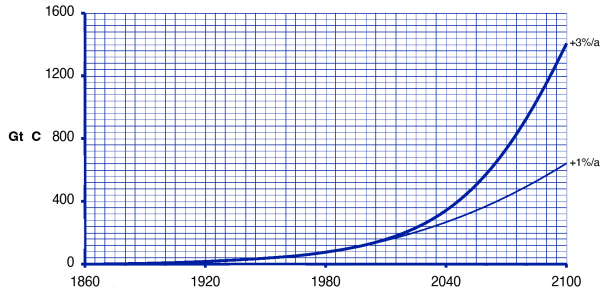

FIGURE 19. The amount of CO_2 absorbed by the entire ocean since 1860 for the trend and low emission scenarios.

This size clearly reflects both changed plant growth and increased soil carbon degradation. Consequently, this calculation variable can also be strongly influenced by possible inaccuracies in the calculation architecture of the carbon cycle model.

A.**10. CO_2 content of the ocean.** The CO_2 content of the entire ocean is reported annually as the variable ASMD (see Figure 19), with the help of the variables ASM and ASD being broken down into the oceanic mixing layer (top 75 m) and the remaining oceanic deep layers. As would be expected, these calculation variables increased continuously from 1860 onwards. Incidentally, the CO_2 content of the world ocean in 1860 is used as the zero point for the numerical representation; it itself amounts to around 40,000 Gt C and is not represented in the graphic representations for reasons of scale.

The oceanic mixed layer (Figure 20) had absorbed around 13 Gt C by 1980; in the trend scenario, this value increases to 77 Gt C by 2050 and to over 220 Gt C by 2100. Diffusion into the deep layers is possible through this mixing layer (into the "deep layers", without illustration): there will be an additional 63 Gt C in 1980, around 370 Gt C by 2050 if the current trend in CO_2 emissions is maintained, and almost 1,200 Gt C by 2100. The uptake of all ocean layers together up to 1980 is around 76 Gt C, which can be related to the value for the sum of fossil emissions to date of 163 Gt C and the phytomass destroyed by deforestation up to that point of around 96 Gt C. According to the CEBM, the ocean has absorbed almost a third of the accumulated anthropogenic emissions to date.

However, in such static numerical estimates based roughly on a year, the temporal CO_2 uptake characteristics of the world ocean must be taken into account: Because of the slowness of the mixing and diffusion processes in the world ocean, a sudden CO_2 emission pulse occurring in the atmosphere can only occur slowly be incorporated into the entire water body of the ocean (Ahamer 2024b, see Figure 14). It is therefore not entirely

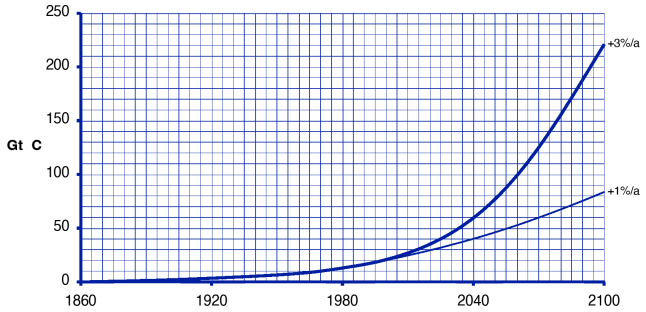

FIGURE 20. The amount of CO_2 absorbed by the entire ocean since 1860 for the trend and low emission scenarios.

unreasonable to extrapolate a percentage found (similar to above) for the ocean uptake of atmospheric CO_2 into the future and increase it as a constant number. In addition, it should be clearly emphasized again that the diffusion model for the ocean used here is a strong simplification, but provides sufficiently useful results for the CEBM.

All important variables issued annually by the CEBM have been discussed now. The following paras are comments on variables that can be output for a year in regional differentiation and are shown in map format in Ahamer (Ahamer 2019, 45–49 and 296–299). Since many such variables change only imperceptibly in their regional differentiation over the decades, they are only shown and discussed for one year. Other variables, which are subject to strong temporal fluctuations, such as clearing activities, are given (on the pages cited above) in time steps of around 40 years.

A.**11. Global distribution of natural phytomass.** Expectably, the density of biomass on natural areas is highest in tropical rainforests. There it is approximately 20,000 grams C/m², which corresponds to 200 t C/ha. The North American east coast as well as Europe and China represent other large carbon reserves. It is recalled that 1 kg of living plant mass corresponds to 0.45 kg of carbon.

To provide guidance on the proportions of the global amounts of carbon stored in living plant mass, the regional distribution of natural phytomass is shown as a pie chart in Figure 21. The legend for the respective hatching of a region is attached. The labelling for regions with a share of <1% is usually removed for reasons of space. In contrast, Figure 22 shows the distribution of the respective land areas. These distributions are listed here in more detail because they represent the starting point for global biomass scenarios and can serve as quantities of plants that can be used for energy.

A.**12. Global distribution of agricultural biomass.** This agricultural biomass is currently concentrated in Europe, the middle latitudes of the former Soviet Union, the eastern USA, China, India and a narrow area in South America (see Figure 23). The population density of up to 200 g C/m² is significantly below that of the natural phytomass because the age of the population in agriculture is assumed to be only one year.

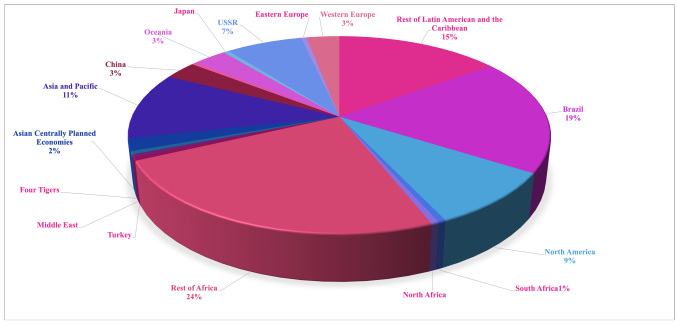

FIGURE 21. The distribution of natural phytomass by 18 world regions including a legend which applies also to the following figures.

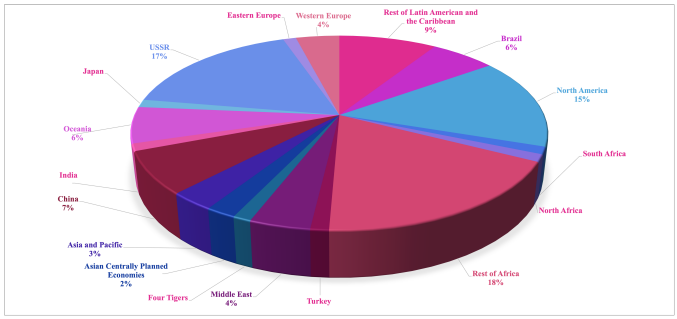

FIGURE 22. The distribution of land area (sum of natural and agricultural use) to 18 world regions.

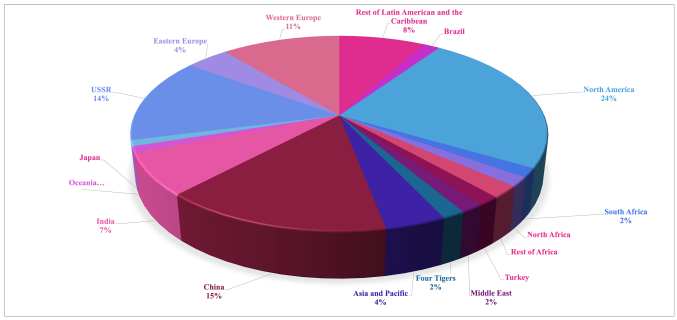

FIGURE 23. Distribution of agricultural phytomass across 18 world regions.

It should be noted that all density values presented here do not represent the theoretically possible vegetation density, but that the latter are already multiplied by the relative area share of the respective land use. For example, if there is a theoretical agricultural vegetation

density of 20 t C/ha in a grid element that is 50% used for agriculture, the corresponding map only shows half of this value.

A.**13. Global distribution of NPP and litter.** Both variables logically show the same geographical distribution as the biomass stock densities (Ahamer 2019, p. 299). The values for the natural NPP in the tropics reach almost up to 1 kg C/m².a, which corresponds to around 22 t of plant mass per hectare per year. The value of around 100 g/m².a (valid in Europe) is due to the very low percentage of natural areas here, but not to any low NPP. The entire agricultural plant mass and part of the natural plant mass (which is indicated by the variable ARATE, describing the herbaceous, non-woody plant content) is to be regarded as herbaceous and therefore easily microbially degradable plant mass. The regional distribution of herbaceous litter is (mathematically) the result of a variety of complex processes: the fluctuation during the so-called pre-run, the clearing processes and other disruptions to the natural carbon cycle such as the fertilization effect (Ahamer 2024a, see Figure 6). This calculation variable therefore reacts sensitively to any inadequacies in the model architecture and therefore only represents a guideline. However, this model result cannot be assigned a level of certainty such as a detailed vegetation zone map experimentally collected through field research. However, it is realistically reflected by the model that the decline in populations, for example in the tropics of Brazil and Central Africa, is very low, which corresponds to the known low litter layer in the rainforests. As expected, the litter layer is low to zero in the desert areas of the world (e.g. Sahara) and in the cold areas. The litter takes on high values, for example, in cool regions with agricultural use, for example in the European part of the ex-Soviet Union. Due to lower temperatures, litter depletion can only take place there to a very limited extent (Figure 24). If you keep in mind that the inflow into the litter compartment is controlled by NPP and the outflow by the litter depletion function described in Ahamer (2022: 31-32), you can see that the filling level of this reservoir depends on the difference between the two flows, which in turn are both a quite complex function of temperature and precipitation. The different curvature of the surfaces in space of these functions therefore influences the final value for the litter compartment resulting from the dynamic flow equilibrium (Figure 24). The woody litter layer, however, shows a very different regional distribution, which consists, for example, of fallen branches and fallen tree trunks. It is very large in a Northern-Eurasia zone and in Canada because microbial degradation there is difficult due to the low temperatures. At least that is the result of the CEBM, which emerged after a settling period of 10,000 model years (Figure 6 in Ahamer, 2024b). In South America and the southern part of Africa, this compartment is also very large because of the high NPP that prevails there.

A.**14. Global distribution of soil organic carbon.** The last one in this series of biospheric carbon reservoirs ultimately derived from photosynthesis is the carbon (SOC) bound in the organic soil components to be discussed (Figure 25). This is the result of very long-lasting exchange processes and is therefore numerically susceptible to weaknesses in the model architecture. As expected, this value is low in the rainforest areas and dry deserts of the world, but high in temperate areas with their well-known thicker soil structure. The regional distribution pattern of this size changes only extremely slowly over the centuries (Ahamer 2024a, see Section 2.3.2). To provide guidance on the current regional distribution of this

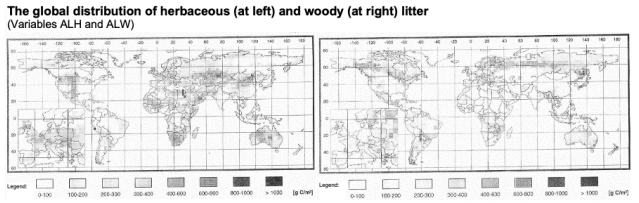

FIGURE 24. The global distribution of herbaceous (at left) and woody (at right) litter for present times in the CEBM.

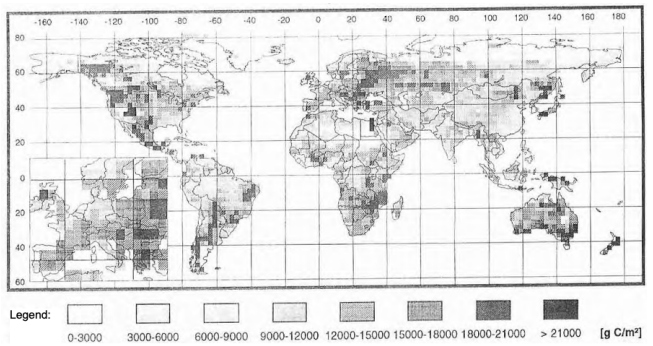

FIGURE 25. The global distribution of soil organic carbon (SOC) litter for present times in the CEBM.

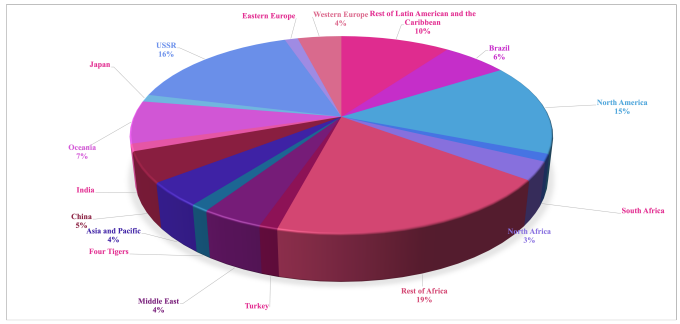

FIGURE 26. Distribution of soil organic carbon across 18 world regions.

largest of all biospheric carbon pools, a diagram with the CEBM model results is shown in Figure 26.

A.**15. Global distribution of deforested phytomass.** During the late 20th century, the deforested areas concentrated on southern Brazil, Indochina and Indonesia as well as scattered places in Africa, but also on the Caribbean (see Figure 27 at left). In many grid elements, up to 10 Mt of carbon (= 22 Mt of biomass) are cleared annually; the

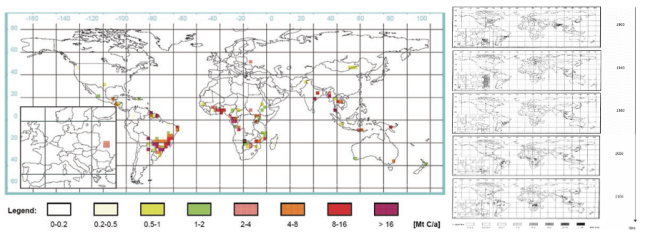

FIGURE 27. The global distribution of deforested biomass at present (left) and as a time series 1900-2100 in steps of half a century (at right).

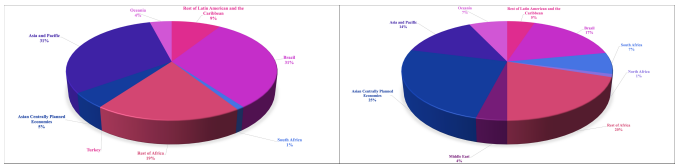

FIGURE 28. Distribution of global deforestation activity (at left) and of the globally deforested area (at right) in 1980 across 18 world regions.

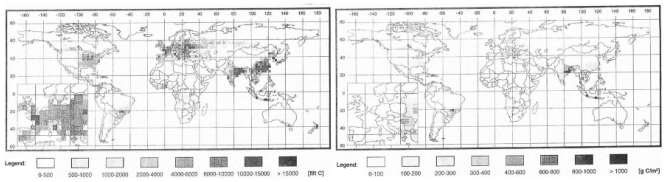

FIGURE 29. Distribution of global deforestation activity (at left) and of the globally deforested area (at right) in 1980 across 18 world regions.

associated CO_2 emissions per grid element even correspond in size to the energy-related CO_2 emissions of small to medium-sized countries. The extremely drastic magnitude of the resulting interference with nature is clearly highlighted. According to the database used, Brazil alone contributed around a third of global deforestation emissions in 1980 (see Figure 28 for deforested biomass, at left, and for deforested areas, at right). These dimensions do call for relief.

In order to make the geographical shift in the focus of clearing activities visible, the clearing maps for the years 1900, 1940, 2050 and 2100 (in the latter years for the moderate clearing scenario) are also shown (see Figure 27 at right). At the turn of the 20th century, the focus of deforestation was in the USA, India and Brazil. During the 21st century, deforestation activity is expected to further spread into the interior of the continents of South America and Africa. The historical total of deforestation from 1860 to 1990 is shown in Figure 29 at right (while, for comparison of geographic distribution, the total of deforestation until 1860 is shown in Figure 29 at left, using a different scale of grey shades).

Unfortunately, the clearing carried out up to 1860 is not directly apparent from the CEBM database. However, an indication of the plant mass destroyed by deforestation from early human history up to 1860 could be obtained by calculating the following numerical value: The natural plant mass that would theoretically be on the areas designated as agricultural in 1860 if they were still naturally covered. This (purely calculation-wise) result is shown at right in Figure 29. Although it can be assumed that this auxiliary quantity represents an overestimation of the clearing activities actually carried out, its high value is extremely striking: if one uses the same grey scale to represent the mentioned quantity and the sum of the biomass cleared from 1860 to 1980 (Ahamer 1993, see Figure A9/41), the map of the latter only shows a few very light grey grid elements. The literature (Esser et al., 1994) also refers to heavy deforestation activities in Europe over the last two millennia. This comparison of mathematical numerical values should be used as an opportunity to point out that the current clearing activities in the Third World must also be seen in the light of the already past and partially forgotten clearing activities in the current First and Second Worlds.

A.**16. Global distribution of net flux from the atmosphere to the biosphere.** The biospheric net emissions are mainly influenced by deforestation activity, which implicitly also includes the previous (mainly unsustainable) traditional energy use of biomass. Compared to 1980 (Figure 30 at below left), the situation around 1900 was still largely balanced (large grey areas in Figure 30 at centre left). The clearing areas at that time (net C release from the biosphere) clearly appear as white spots, while heavily overgrown areas without clearing activity (untouched virgin forest) appear slightly dark due to the net C uptake by the biosphere due to the CO_2 fertilizer effect, which is already becoming somewhat effective at elevated CO_2 concentration levels (Figure 30 at right).

The play of grey shades described becomes much more pronounced around 1940 or later (Figure 30 at left) and continues into the 21st century (Figure 30 at right). The bright areas corresponding to deforestation emissions can be seen most clearly here. In the literature (Nakićenović et al., 1992), even stronger deforestation scenarios are sometimes assumed compared to the CEBM.

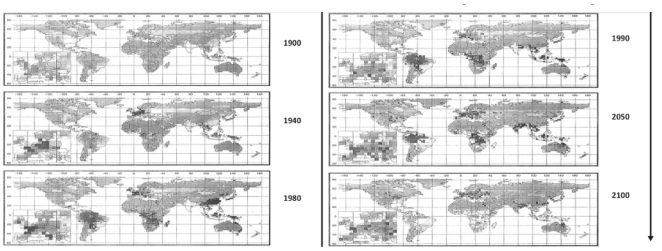

FIGURE 30. Distribution of global deforestation activity (at left) andThe global distribution of the carbon "balance" as a time series 1900-2100 in steps of half a century (at right); compare the timeline in Figure 17, and the legend in Figure 18.

The above-mentioned descriptions in the sections A.1 to A.16 of the annex additionally describe the systems dynamics characteristic for the global carbon pools and fluxes and therefore allow the assessment that the CEBM is a valid tool to assess the planet-wide usage of biomass for energy, and to trust in the results showing the net CO_2 concentration in the atmosphere.

Acknowledgments

The author thanks colleagues at Joanneum Research and the Austrian Ministry of Science and Research as well as from the EU Escoba project for valuable discussions.

References

Abbasi, T. and Abbasi, S. A. (2010). "Biomass energy and the environmental impacts associated with its production and utilization". *Renewable and Sustainable Energy Reviews* **14**(3), 919–937. DOI: 10.1016/j.rser.2009.11.006.

Ackerman, F., DeCanio, S. J., Howarth, R. B., and Sheeran, K. (2009). "Limitations of integrated assessment models of climate change". *Climatic Change* **95**(3-4), 297–315. DOI: 10.1007/s10584-009-9570-x.

Ahamer, G. (1993). "Der Einfluss einer verstärkten energetischen Biomassenutzung auf die CO2-Konzentration in der Atmosphäre". Available at https://www.researchgate.net/publication/319130468. PhD thesis. Graz University of Technology.

Ahamer, G. (2019). *Mapping Global Dynamics – Geographic Perspectives from Local Pollution to Global Evolution*. Dordrecht, The Netherlands: Springer International Publishing. DOI: 10.1007/978-3-319-51704-9.

Ahamer, G. (2022). "Why Biomass Fuels Are Principally Not Carbon Neutral". *Energies* **15**, 9619. DOI: 10.3390/en15249619.

Ahamer, G. (2024a). "Carbon cycle models quantify for a green and low-carbon economy". *Green and Low-Carbon Economy*. DOI: 10.47852/bonviewGLCE42022240.

Ahamer, G. (2024b). "How to compute whether biomass fuels are carbon neutral". *ournal for carbon research* **10**, 48 [27 pages].

Ahamer, G., Fankhauser, G., Spitzer, J., and Weiss, C.-O. (1991). *Der Einfluss einer verstärkten energetischen Biomassenutzung auf die CO2-Konzentration in der Atmosphäre*. DOI: 10.13140/RG.2.2.14359.88486.

Akimoto, K., Tomoda, T., Fujii, Y., and Yamaji, K. (2004). "Assessment of global warming mitigation options with integrated assessment model DNE21". *Energy Economics* **26**(4), 635–653. DOI: 10.1016/j.eneco.2004.04.021.

Azar, C., Lindgren, K., Larson, E., and Möllersten, K. (2006). "Carbon capture and storage from fossil fuels and biomass - costs and potential role in stabilizing the atmosphere". *Climatic Change* **74**(1-3), 47–79. DOI: 10.1007/s10584-005-3484-7.

BMHGI (1984). *Österreichischer Energiebericht*. Energiebericht und Energiekonzept 1984 der Österreichischen Bundesregierung, Bundesministerium für Handel, Gewerbe und Industrie, Sektion Energie, Wien.

Boykova, M., Knyazeva, H., and Salazkin, M. (2023). "History and Modern Landscape of Futures Studies". *Foresight and STI Governance* **17**(4), 80–91. DOI: 10.17323/2500-2597.2023.4.80.91.

Carlson, K. M., Curran, L. M., Asner, G. P., Pittman, A. M., Trigg, S. N., and Marion Adeney, J. (2013). "Carbon emissions from forest conversion by Kalimantan oil palm plantations". *Nature Climate Change* **3**(3), 283–287. DOI: 10.1038/nclimate1702.

Chen, Y., Lewis, N. S., and Xiang, C. (2015). "Operational constraints and strategies for systems to effect the sustainable, solar-driven reduction of atmospheric CO2". *Energy and Environmental Science* **8**(12), 3663–3674. DOI: 10.1039/c5ee02908b.

Chester, M. V., Horvath, A., and Madanat, S. (2010). "Comparison of life-cycle energy and emissions footprints of passenger transportation in metropolitan regions". *Atmospheric Environment* **44**(8), 1071–1079. DOI: 10.1016/j.atmosenv.2009.12.012.

Claret, M., Sonnerup, R. E., and Quay, P. D. (2021). "A next generation ocean carbon isotope model for climate studies I: Steady state controls on ocean 13C". *Global Biogeochemical Cycles* **35**(4). DOI: 10.1029/2020GB006757.

Danielsen, F., Beukema, H., Burgess, N. D., Parish, F., Brühl, C. A., Donald, P. F., *et al.* (2009). "Biofuel plantations on forested lands: Double jeopardy for biodiversity and climate". *Conservation Biology* **23**(2), 348–358. DOI: 10.1111/j.1523-1739.2008.01096.x.

Demirbas, A. (2004). "Combustion characteristics of different biomass fuels". *Progress in Energy and Combustion Science* **30**(2), 219–230. DOI: 10.1016/j.pecs.2003.10.004.

Esser, G. (1984). "The Significance of Biospheric Carbon Pools and Fluxes for the Atmospheric CO2: A Proposed Model Structure". *Progress in Biometeorology* **3**, 253–294.

Esser, G. (1987). "Sensitivity of Global Carbon Pools and Fluxes to Human and Potential Climatic Impacts". *Tellus*. B **39**, 245–260.

Esser, G. (1988). "Global Land Use Changes from 1860 to 1980 and Future Projections to 2500". *Ecological Modelling* **44**(3-4), 307–316.

Fitzherbert, E. B., Struebig, M. J., Morel, A., Danielsen, F., Brühl, C. A., Donald, P. F., and Phalan, B. (2008). "How will oil palm expansion affect biodiversity?" *Trends in Ecology and Evolution* **23**(10), 538–545. DOI: 10.1016/j.tree.2008.06.012.

Green, J. and Reyes, R. (2023). "The history of net zero: can we move from concepts to practice?" *Climate Policy* **23**(7), 901–915. DOI: 10.1080/14693062.2023.2218334.

Gunatilake, H., Roland-Holst, D., and Sugiyarto, G. (2014). "Energy security for India: Biofuels, energy efficiency and food productivity". *Energy Policy* **65**, 761–767. DOI: 10.1016/j.enpol.2013.10.050.

Gürdil, G., Demirel, B., and Cevher, E. (2024). "The conceptualization of agricultural residues: unlocking potential for sustainability". *BIO Web Conf.* **85**, 01068. DOI: 10.1051/bioconf/20248501068.

Intergovernmental Panel on Climate Change (IPCC) (1991). *Potential Impacts of Climate Change*. Report prepared for the International Panel on Climate Change by Working Group I, II, III, World Meteorological Organization (WMO) and United Nations Environmental Program (UNEP). URL: https://www.ipcc.ch.

Intergovernmental Panel on Climate Change (IPCC) (2000). *Special Report on Emission Scenarios*. Summary for Policy Makers; International Panel for Climate Change—IPCC: Geneva, Switzerland. URL: https://www.ipcc.ch/site/assets/uploads/2018/03/sres-en.pdf.

Intergovernmental Panel on Climate Change (IPCC) (2021). *Sixth Assessment Report*. IPCC Working Group I. URL: https://www.ipcc.ch/assessment-report/ar6/.

Intergovernmental Panel on Climate Change (IPCC) (2023). *Sixth Assessment Report*. IPCC Working Group I. URL: https://www.ipcc.ch/report/sixth-assessment-report-cycle/.

Koh, L. P., Miettinen, J., Liew, S. C., and Ghazoul, J. (2011). "Remotely sensed evidence of tropical peatland conversion to oil palm". *Proceedings of the National Academy of Sciences of the United States of America* **108**(12), 5127–5132. DOI: 10.1073/pnas.1018776108.

Körner, C. (2006). "Plant CO2 responses: An issue of definition, time and resource supply". *New Phytologist* **172**(3), 393–411. DOI: 10.1111/j.1469-8137.2006.01886.x.

Kraxner, F., Nilsson, S., and Obersteiner, M. (2003). "Negative emissions from BioEnergy use, carbon capture and sequestration (BECS) - the case of biomass production by sustainable forest

management from semi-natural temperate forests". *Biomass and Bioenergy* **24**(4-5), 285–296. DOI: 10.1016/S0961-9534(02)00172-1.

Kukharets, S., Jasinskas, A., Golub, G., Sukmaniuk, O., Hutsol, T., Mudryk, K., Česna, J., Glowacki, S., and Horetska, I. (2023). "The Experimental Study of the Efficiency of the Gasification Process of the Fast-Growing Willow Biomass in a Downdraft Gasifier". *Energies* **16**(2), 578. DOI: 10.3390/en16020578.

Le, T., Sharma, P., Le, H., Le, H., Osman, S., Truong, T., Le, D., Rowinski, L., and Tran, V. (2024). "A glass-box approach for predictive modeling based on experimental data for a waste biomass derived producer gas-powered dual-fuel engine". *International Journal of Hydrogen Energy* **58**, 1122–1137. DOI: 10.1016/j.ijhydene.2024.01.284.

Makky, A. A., Alaswad, A., Gibson, D., and Olabi, A. G. (2017). "Renewable energy scenario and environmental aspects of soil emission measurements". *Renewable and Sustainable Energy Reviews* **68**, 1157–1173. DOI: 10.1016/j.rser.2016.05.088.

Moumen, A., Azizi, G., Chekroun, K. B., and Baghour, M. (2016). "The effects of livestock methane emission on the global warming: A review". *International Journal of Global Warming* **9**(2), 229–253. DOI: 10.1504/IJGW.2016.074956.

Muench, S. and Guenther, E. (2013). "A systematic review of bioenergy life cycle assessments". *Applied Energy* **112**, 257–273. DOI: 10.1016/j.apenergy.2013.06.001.

Nastasi, B., Markovska, N., Puksec, T., Duić, N., and Foley, A. (2023). "Techniques and technologies to board on the feasible renewable and sustainable energy systems". *Renewable and Sustainable Energy Reviews* **182**, art. no. 113428. DOI: 10.1016/j.rser.2023.113428.

Nickerson, N. and Risk, D. (2009). "Physical controls on the isotopic composition of soil-respired CO2". *Journal of Geophysical Research: Biogeosciences* **114**(1). DOI: 10.1029/2008JG000766.

Nordhaus, W. (2011). "Designing a friendly space for technological change to slow global warming". *Energy Economics* **33**(4), 665–673. DOI: 10.1016/j.eneco.2010.08.005.

Notter, D. A., Meyer, R., and Althaus, H. (2013). "The western lifestyle and its long way to sustainability". *Environmental Science and Technology* **47**(9), 4014–4021. DOI: 10.1021/es3037548.

Pan, M., Aziz, F., Li, B., Perry, S., Zhang, N., Bulatov, I., and Smith, R. (2016). "Application of optimal design methodologies in retrofitting natural gas combined cycle power plants with CO2 capture". *Applied Energy* **161**, 695–706. DOI: 10.1016/j.apenergy.2015.03.035.

Pereira Jr., A. O., Pereira, A. S., La Rovere, E. L., Barata, M. M. D. L., Villar, S. D. C., and Pires, S. H. (2011). "Strategies to promote renewable energy in Brazil". *Renewable and Sustainable Energy Reviews* **15**(1), 681–688. DOI: 10.1016/j.rser.2010.09.027.

Podolets, R., Diachuk, O., Semeniuk, A., Serebrennikov, B., Trypolska, G., Yuhymets, R., and Yevstihnieieva, O. (2023). *Rebuilding Ukraine with a Resilient, Carbon-Neutral Energy System*. UNECE. URL: https://unece.org/sustainable-energy/publications/rebuilding-ukraine-resilient-carbon-neutral-energy-system.

Rittmann, B. E. (2008). "Opportunities for renewable bioenergy using microorganisms". *Biotechnology and Bioengineering* **100**(2), 203–212. DOI: 10.1002/bit.21875.

Röös, E., Sundberg, C., Tidåker, P., Strid, I., and Hansson, P. (2013). "Can carbon footprint serve as an indicator of the environmental impact of meat production?" *Ecological Indicators* **24**, 573–581. DOI: 10.1016/j.ecolind.2012.08.004.

Sahin, Y. (2011). "Environmental impacts of biofuels". *Energy Education Science and Technology Part A: Energy Science and Research* **26**(2), 129–142.

Sahni, T., Verma, D., and Kumar, S. (2024). "Biochar: A Pyrolyzed Green Fuel from Paddy Straw". In: *Paddy Straw Waste for Biorefinery Applications. Clean Energy Production Technologies*. Ed. by N. Srivastava, B. Verma, and P. Mishra. Singapore: Springer. DOI: 10.1007/978-981-99-8224-0_10.

Schlamadinger, B., Spitzer, J., Kohlmaier, G. H., and Lüdeke, M. (1995). "Carbon balance of bioenergy from logging residues". *Biomass and Bioenergy* **8**(4), 221–234. DOI: 10.1016/0961-9534(95)00020-8.

Spitzer, J. (1990). *Gegenüberstellung energiewirtschaftlicher Empfehlungen zur Verwirklichung der energiepolitischen Ziele bei der Raumwärmeversorgung*. Universitätsverlag Leuschner und Lubensky, Graz, Austria.

Spitzer, J. (1991). *Worldwide availability of today's and tomorrow's energy sources*. Information service "Energy and Environment": Reports from research and practice in Austria, No. 2, ed. Interuniversity Research Institute for Distance Learning, Klagenfurt Study Center, October 1990.

Suberu, M. Y., Bashir, N., and Mustafa, M. W. (2013). "Biogenic waste methane emissions and methane optimization for bioelectricity in Nigeria". *Renewable and Sustainable Energy Reviews* **25**, 643–654. DOI: 10.1016/j.rser.2013.05.017.

Tran, H., Juno, E., and Arunachalam, S. (2023). "Emissions of wood pelletization and bioenergy use in the United States". *Renewable Energy* **219**, art. no. 119536. DOI: 10.1016/j.renene.2023.119536.

Tregub, O. (2023). "Preferential taxation of carbon dioxide emissions from biofuel burning in the context of reassessment of the impact of bioenergy on the climate". *Economy and law* (2), 43–51. DOI: 10.15407/econlaw.2023.02.043.

Wang, Y. P., Law, R. M., and Pak, B. (2010). "A global model of carbon, nitrogen and phosphorus cycles for the terrestrial biosphere". *Biogeosciences* **7**(7), 2261–2282. DOI: 10.5194/bg-7-2261-2010.

Weiss, M., Patel, M., Heilmeier, H., and Bringezu, S. (2007). "Applying distance-to-target weighing methodology to evaluate the environmental performance of bio-based energy, fuels, and materials". *Resources, Conservation and Recycling* **50**(3), 260–281. DOI: 10.1016/j.resconrec.2006.06.003.

White, G. (2012). *Climate change and migration: Security and borders in a warming world*. DOI: 10.1093/acprof:oso/9780199794829.001.0001.

Wieder, W. R., Boehnert, J., and Bonan, G. B. (2014). "Evaluating soil biogeochemistry parameterizations in earth system models with observations". *Global Biogeochemical Cycles* **28**(3), 211–222. DOI: 10.1002/2013GB004665.

* Graz University, Global Studies,
Global Studies, Macherstrasse 15
8047, Graz, Austria

Email: gilbert.ahamer@chello.at

Paper contributed to the international conference on
"Atmospheric Monitoring, Modeling and Simulation", held in Messina, Italy (2-3 December 2019)
under the patronage of the *Accademia Peloritana dei Pericolanti*

Manuscript received 9 September 2022; published online 1 October 2025